2-Pyrrolinodoxorubicin and its peptide-vectorized form bypass multidrug resistance

Cédric Castex[a], Peggy Merida[b], Emmanuelle Blanc[b], Philippe Clair[a], Anthony R. Rees[a,c] and Jamal Temsamani

A well-known mechanism leading to the emergence of multidrug-resistant tumor cells is the overexpression of P-glycoprotein, which is capable of lowering intracellular drug concentrations. In the present study, we tested the capability of 2-pyrrolinodoxorubicin (p-DOX), a highly potent derivative of DOX, to bypass multidrug resistance. The accumulation, intracellular distribution and cytotoxicity of p-DOX were tested in two cell lines (K562 and A2780) and their DOX-resistant counterparts (K562/ADR and A2780/ADR). Cellular accumulation and cytotoxicity were dramatically lowered for DOX in resistant cell lines, in comparison with non-resistant cells. In contrast, cellular accumulation, intracellular distribution and cytotoxicity of p-DOX were independent of the nature of the cell lines. The p-DOX showed potent dose-dependent inhibition of cell growth against resistant cells as compared with DOX. After treatment of resistant cells with verapamil, the intracellular levels of DOX were markedly increased and consequent cytotoxicity improved. In contrast, treatment of resistant cells with verapamil did not cause any further enhancement of cell uptake or an increase in the cytotoxic effect of the derivative p-DOX, indicating that the compound bypasses the P-glycoprotein. Finally, we show that vectorization of p-DOX by a peptide vector (SynB3) which has been shown to enhance the brain uptake of DOX and to decrease its heart accumulation does not affect this property. These results indicate that p-DOX and its vectorized form are potent and effective in overcoming multidrug resistance. *Anti-Cancer Drugs* 15:609–617
© 2004 Lippincott Williams & Wilkins.

Anti-Cancer Drugs 2004, **15**:609–617

Keywords: 2-pyrrolinodoxorubicin, doxorubicin, multidrug resistance, peptide conjugate, P-glycoprotein

[a]Synt:em, Parc Scientifique Georges Besse, 30000 Nîmes, France and [b]Synt:em, Institut de Génétique Moléculaire de Montpellier, CNRS UMR 5535, 1919 Route de Mende, 34293 Montpellier Cedex 5, France.
[c]Present address: MIP Technologies AB, Research Park Ideon, 223 70 Lund, Sweden.

Correspondence to J. Temsamani, Synt:em, Parc Scientifique Georges Besse, 30000 Nîmes, France.
Tel: +33 4 6604 8666; fax: +33 4 6604 8667;
e-mail: jtemsamani@syntem.com

Received 3 February 2004 **Revised form accepted** 27 February 2004

Introduction

The resistance of certain human tumors to chemotherapeutic agents is one of the main problems currently encountered in the struggle against cancer. This resistance is often the consequence of a first treatment with an anticancer drug. After the first administrations, cancerous cells begin to overexpress efflux proteins which are directly involved in the chemoresistance of the tumors to anticancer agents. The consequences of such an overexpression are to limit the uptake of the agent or to increase its drug excretion out of the tumor. Two of these efflux proteins have been particularly well studied. The first, P-glycoprotein (P-gp), is a 170-kDa ATP-dependent efflux pump [1]. P-gp functions as an ATP-driven pump capable of removing the drugs from the cytoplasm and consequently lowering the drug concentration inside the cell [2]. It has been demonstrated that P-gp is also present at the luminal site of the endothelial cells of the blood–brain barrier (BBB) [3]. As a consequence of P-gp expression at the BBB interface and overexpression within brain tumors, the bioavailability of anticancer agents is extremely low explaining the failure of brain tumor chemotherapy. A second type of efflux protein that has also been implicated in the multidrug resistance phenomenon is the MRP protein [4].

To overcome multidrug resistance within brain tumors, different approaches have been taken. Strategies that enhance penetration through the BBB are usually invasive, requiring methods such as intraventricular drug infusion or disruption of the BBB [5,6]. Other approaches have attempted to block the P-gp activity and where chemotherapeutic agents are administered in combination with P-gp inhibitors such as cyclosporine [7], verapamil (VPL) [8], tamoxifen [9] or PSC 833 [10]. These methods have been proven to be effective *in vitro*, but the high concentrations of inhibitors necessary to circumvent the P-gp activity *in vivo* limit their clinical use.

Alternative strategies, such as drug vectorization, have also been developed to limit drug efflux from the cancerous cells. A number of chemotherapeutic agents have been linked to proteins [11–14], monoclonal antibodies [15–18], polymers [19–25], particles or cationic lipids [26–29] and cyclodextrins [30].

0959-4973 © 2004 Lippincott Williams & Wilkins DOI: 10.1097/01.cad.0000132231.28888.fa

Copyright © Lippincott Williams & Wilkins. Unauthorized reproduction of this article is prohibited.

Although such covalently linked 'adjuvants' have provided some benefits, such as reduction in toxicity or better delivery of the cytotoxic agent, the drawback caused by the relatively large size of the vectors has hindered their clinical use.

Recently, we have shown that the use of small peptide vectors, such as SynB vectors, can enhance the brain uptake of various drugs including anticancer agents. For one such agent, doxorubicin (DOX), this enhancement is accompanied by a decrease in its accumulation in heart, where it exerts its toxic effect [31–33]. We have also shown that vectorized DOX bypasses the P-gp, both *in vitro* and *in vivo* [34].

Another way to circumvent the multidrug resistance or the side-effects of some anticancer agents was to synthesize semi-synthetic derivatives of these chemotherapeutic agents. Several analogs of DOX have led to powerful cytotoxic agents with limited systemic toxicity including the 3-cyanomorpholino-DOX [35–39].

More recently, 2-pyrrolino-DOX (p-DOX) has been proven to be more than 500-fold more potent than DOX on different cell lines [40]. This analog possesses a pyrrolino ring which includes the nitrogen of the daunosamine moiety of DOX which has been shown to be responsible for the enhanced activity of the compound after a structure–activity study based on a set of derivatives. p-DOX was also used in combination with various peptides in order to target its cytotoxic activity against cells equipped with membrane receptors [41–45]. However, the activity of p-DOX against cells expressing P-gp or MRP was not investigated.

In the present study, we investigated the internalization and cell cytotoxicity of p-DOX against two resistant cell lines (K562 and A2780 cells) overexpressing the P-gp pump. We also present preliminary results concerning the use of a peptide conjugate of p-DOX.

Materials and methods

Materials

2-(3-Chloropropyl)-1,3-dioxolane, DOX hydrochloride, *N*,*N*-diisopropylethylamine (DIEA) and piperidin were purchased from Fluka (St Quentin Fallavier, France). Dimethylformamide (DMF), acetonitrile (ACN), diethyl ether, acetic acid and succinic anhydride were purchased from Sigma-Aldrich (St Quentin Fallavier, France). 9-Fluorenylmethoxycarbonyloxysuccinimid (Fmoc-OSu) and (benzotriazol-1-yloxy)tripyrrolidinophosphonium (PyBOP) were obtained from Novabiochem (Limonest, France). Prior to use, DMF was placed on a 3-Å molecular sieve for 24 h (extruders 1.6 mm; Prolabo, Lyon, France).

Analytical HPLC were performed on a Beckman Gold 32 Karat System, with a Waters Symmetry Shield C_{18} column (250 × 4.6 mm; 5 m) using the following solvent system A = H_2O/0.1% TFA and B = ACN/0.1% TFA. A Waters preparative system equipped with Prep LC Novapack C_{18} cartridges (40 × 4.6 mm; 6 m; 60 Å) was used for preparative HPLC with the same solvent system. MALDI-TOF analysis was performed on a Voyager Elite XL System spectrometer (Perseptive Biosystems, Voisins le Bretonneux, France) and LC/MS/MS mass analysis realized on a quadripolar MicroMass Quattro Ultima spectrometer.

Cell lines

K562 (human erythroleukemia), A2780 (ovarian carcinoma) and K562/ADR were supplied by ATCC (Rockville, MD). A2780/ADR were from ECACC (Salisbury, UK). Resistant cells K562/ADR and A2780/ADR derived from the parental cell lines by sequential selections for DOX resistance. Cells were cultivated as described by the supplier, and were grown in RPMI medium supplemented with 10% fetal calf serum (v/v) and glutamax (Gibco Invitrogen, Cergy Pontoise, France).

Synthesis

Peptide synthesis

Peptide was assembled by conventional solid-phase chemistry using a 9-fluorenylmethoxycarbonyl/tertiobutyl (Fmoc/tBu) protection scheme [46]. The crude peptide was purified on C_{18} reverse-phase preparative HPLC after trifluoroacetic acid cleavage/deprotection. The purity of peptide was assessed by C_{18} reverse-phase analytic HPLC and MALDI-MS. The peptide sequence was SynB3 (RRLSYSRRRF; 1395 Da).

4-Iodobutyraldehyde (product 1)

The synthesis of 4-iodobutyraldehyde was realized as described by Nagy *et al.* [40]. Briefly, 2-(3-chloropropyl)-1,3-dioxolane (1.32 ml; 10 mmol) was added to a solution containing sodium iodide (30 g; 200 mmol) in 20 ml acetone. The solution was refluxed for 24 h. Acetone was evaporated to dryness and 100 ml of diethyl ether were added to the white residue. After filtration, the organic layer was washed successively with 50 ml of water, 50 ml of a 5% sodium thiosulfate solution (w/v) and 3 times with 50 ml of water. Diethyl ether was evaporated and 3 ml of a 50% acetic acid solution (v/v) was added to the yellow oil obtained. The solution was stirred for 1 h and 100 ml of diethyl ether was added. The organic layer was washed with water until neutral pH was reached and dried over $MgSO_4$. After evaporation of diethyl ether, the yellow oily residue which gave a yellow spot on TLC with 2,4-dinitrophenylhydrazine was used without further purification for the synthesis of p-DOX.

p-DOX (product 2)

To a solution containing DOX hydrochloride (290 mg; 0.5 mmol) and DIEA (342 µl; 2 mmol) in 12.8 ml of dry DMF was added dropwise 2.96 g (15 mmol) of crude

Copyright © Lippincott Williams & Wilkins. Unauthorized reproduction of this article is prohibited.

4-iodobutyraldehyde. The solution was stirred for 15 min in the dark at room temperature. Then, 120 ml of a solution containing ACN/H_2O/acetic acid (70/28/2; v/v/v) was added and two extractions by 50 ml of hexane were made to eliminate the excess of 4-iodobutyraldehyde. After dilution with 700 ml of H_2O (TFA 0.1%; v/v)/ACN (TFA 0.08%; v/v) (90/10; v/v), the red solution was applied on a C_{18} reverse-phase preparative HPLC (from 5 to 90% of buffer B in 60 min). The fractions containing p-DOX were pooled and lyophilized to yield 21909 mg (yield: 74%) of a 98% pure intense red powder. MALDI MS: m/e [HABA] 596.1 ($M + H^+$). Calculated exact mass: 595.61 g/mol. SM ES^+: m/e 596,7 $[M + H]^+$; 398.1 (adriamycinone); 361.2; 321.0.

N-*9-fluorenylmethoxycarbonyl-DOX (product 3)*

Doxorubicin hydrochloride (302 mg; 0.52 mmol) was suspended in 6 ml of dry DMF. DIEA (177 µl; 1.04 mmol) was added followed by a solution of Fmoc-OSu (526 mg; 1.56 mmol) in 2 ml of dry DMF. The solution was stirred for 30 min at room temperature. Diethyl ether (100 ml) was added and the red precipitate was isolated by centrifugation. The red solid was washed twice by 100 ml diethyl ether and after drying under vacuum was purified on a C_{18} reverse-phase preparative HPLC (from 5 to 90% of buffer B in 60 min). The fractions containing the desired product were pooled and lyophilized to give 313 mg (yield 79%) of a 98% pure red powder. MALDI MS: m/e [HABA] 766.83 ($M + H^+$). Calculated exact mass: 765.78 g/mol.

N-*9-fluorenylmethoxycarbonyl-14-*O*-succinyl-DOX (product 4)*

A sample of 300 mg (0.39 mmol) of product **3** was dissolved in 3 ml of dry DMF. Solutions containing respectively 171 mg (2 mmol) of lithium bromide in 1.71 ml of dry DMF, 197 mg (2 mmol) of succinic anhydride in 1.97 ml of dry DMF and 268 µl (1.57 mmol) of DIEA were successively added. The solution was stirred in the dark 24 h. The reaction was quenched by adding dropwise 800 µl of glacial acetic acid and *N*-9-fluorenylmethoxycarbonyl-14-*O*-succinyl-DOX was precipitate by addition of 100 ml of diethyl ether. After centrifugation, the red precipitate was washed twice with 100 ml of diethyl ether and applied on a C_{18} reverse-phase preparative HPLC (from 15% to 90% of buffer B in 60 min). The fractions containing the desired product were pooled and lyophilized to give 268 mg (yield: 79%) of a 98% pure red powder. MALDI MS: m/e [HABA] 867.03 ($M + H^+$). Calculated exact mass: 865.85 g/mol.

*(N-9-fluorenylmethoxycarbonyl-14-*O*-succinyl-Arg-Arg-Leu-Ser-Tyr-Ser-Arg-Arg-Arg-Phe-NH_2)-DOX (product 5)*

To a solution of compound **4** (200 mg; 0.23 mmol) in 2 ml of dry DMF was added successively a solution containing the peptide (451 mg; 0.32 mmol) in 3 ml of dry DMF, 134 mg (0.25 mmol) of PyBOP and 79 µl (0.46 mmol) of DIEA. The solution was stirred for 50 min and the conjugate was precipitated by addition of 50 ml of diethyl ether. The red precipitate was isolated by centrifugation, washed twice with 50 ml of diethyl ether and purified with a C_{18} reverse-phase preparative HPLC (from 15 to 90% of buffer B in 60 min). The fractions containing the desired product were lyophilized to yield 346 mg (yield: 67%) of a 98% pure red powder. MALDI MS: m/e [HABA] 2246.65 ($M + H^+$). Calculated exact mass: 2243.49 g/mol.

*(14-*O*-succinyl-Arg-Arg-Leu-Ser-Tyr-Ser-Arg-Arg-Arg-Phe-NH_2)-DOX (product 6)*

A sample of 100 mg of compound 5 (42.5 µmol) was dissolved in 2 ml of dry DMF, then 83.9 µl. of piperidin was added and the solution was stirred for 10 min. The reaction was quenched by adding 500 µl of glacial acetic acid and then 50 ml of diethyl ether was added. After centrifugation, the precipitate obtained was washed twice with 50 ml of diethyl ether and applied on a C_{18} reverse-phase preparative HPLC (from 15 to 90% of buffer B in 60 min). The fractions of interest were pooled and lyophilized to give 62 mg (yield: 73%) of 98% pure 14-*O*-succinyl-Arg-Arg-Leu-Ser-Tyr-Ser-Arg-Arg-Arg-Phe-NH_2)-DOX as a red powder. MALDI MS: m/e [HABA] 2023.18 ($M + H^+$), 2045.55 ($M + Na^+$), 2060.78 ($M + K^+$). Calculated exact mass: 2021,24 g/mol.

*(14-*O*-succinyl-Arg-Arg-Leu-Ser-Tyr-Ser-Arg-Arg-Arg-Phe-NH_2)-p-DOX (product 7)*

A sample of 55 mg of compound **6** (27.2 µmol) was dissolved in 800 µl of dry DMF. Then, 18.6 µl (10^9 µmol) of DIEA and 162 mg (816 µmol) of 4-iodobutyraldehyde dissolved in a minimum of dry DMF were added. The reaction mixture was stirred for 15 min and diluted with a solution of H_2O/TFA (0.1%) q.s.p. 50 ml. After centrifugation, the supernatant was injected on a C_{18} reverse-phase preparative HPLC (from 15 to 90% of buffer B in 60 min).

The fractions containing the final product were pooled and lyophilized to yield 46.2 mg (yield: 82%) of 98% pure (14-*O*-succinyl-Arg-Arg-Leu-Ser-Tyr-Ser-Arg-Arg-Arg-Phe-NH_2)-p-DOX as a red powder. MALDI MS: m/e [HABA] 2075.54 ($M + H^+$), 2098.26 ($M + Na^+$). Calculated exact mass: 2073.32 g/mol.

Cytotoxicity assay

Cytotoxicity of p-DOX, p-DOX-SynB3 and DOX was assessed by the colorimetric MTT assay. Briefly, cells were seeded at 10^4 cells/well in a 96-well plate in Opti-MEM (Gibco, Cergy Pontoise, France) 24 h before the incubation, for 48 h, with increasing concentrations of drugs. After this time, 0.5 mg/ml MTT (Sigma, St Quentin Fallavier, France) was added to each well and cells were incubated for another 4 h at 37°C. Medium was

Copyright © Lippincott Williams & Wilkins. Unauthorized reproduction of this article is prohibited.

then removed and cells and formazan crystals were solubilized in a DMF/SDS solution. Absorbance at 550 nm was determined by a Spectrafluor Plus Tecan plate reader. The E_{max}, the maximal cell death induced by the drug, and the IC_{50}, the drug concentration inducing 50% of E_{max}, were determined by plotting absorbance against log drug concentration. Each experiment was carried out 6 times and was repeated at least 3 times independently.

Quantification of internalization of DOX, p-DOX or p-DOX-SynB3

Internalization of DOX, p-DOX and p-DOX-SynB3 into K562 and K562/ADR was assessed by flow cytometry. K562 cells were diluted at 3×10^5 cells/ml in culture medium 1 day before the experiment. Cell association and internalization of peptides were measured by flow cytometry using a FACSCalibur (Becton Dickinson, Le Pont de Claix, France) driven with CellQuest software. The flow cytometer was periodically calibrated using fluorescent beads (Calibrite3; BD Bioscience). The day of the experiment, cells were counted, centrifuged and resuspended in pre-warmed Opti-MEM (37°C) to obtain a suspension at 6×10^5 cells/ml. After 1 h equilibration, drugs were incubated with K562 cells in the same medium at 37°C for 90 min (final volume 0.5 ml). Thereafter, the cells were washed twice and resuspended in 0.5 ml (final volume) of ice-cold PBS for flow cytometry analysis.

About 400 000 adherent cells lines were plated 24 h before on 12-wells plate in 2 ml of complete medium. The day of the experiment, cells were pre-warmed in Opti-MEM. After 1 h of equilibration, drugs were incubated with cells in the same medium at 37°C for 90 min (final volume 0.5 ml). Thereafter, cells were washed twice with ice-cold PBS and trypsinized 5 min at 37°C. Reaction was stopped by 0.5 ml of complete medium, and cells were transferred in FACS tubes, washed and resuspended in 0.5 ml of ice-cold PBS for flow cytometry analysis.

Internalized drugs were excited at 488 nm and fluorescence was measured at 525 nm. A histogram of fluorescence intensity per cell (1×10^4 counts) was obtained and the calculated mean of this distribution was considered as representative of the amount of intracellular antineoplastic agent.

Confocal microscopy

Adherent A2780 cell lines were plated 24 h before on glass slides. Drugs (25 μM) were incubated with K562, K562/ADR, A2780 or A2780/ADR cells in Opti-MEM medium at 37°C for 90 min.Thereafter, the cells were washed twice with ice-cold PBS and resuspended in 20 μl (final volume) of the same buffer. Suspensions of K562 cell lines were plated on glass slides and immediately observed without fixation. Confocal images were obtained with a DMR-B Leica microscope equipped with an Ar-Kr ion laser with excitation at 488 nm and emission at 525 nm, and fitted with a Perkin-Elmer Ultraview module (Bracknell, UK). The image captured with a CoolSnap HQ camera (Photometrics, Huntington Beach, CA) at 696×520 pixel resolution. The whole set was controlled with the MetaMorph software (Universal Imaging, Downingtown, PA). The samples were observed with a $\times 40$ oil immersion PL AZO HCX lens.

Results

Cell internalization of p-DOX and DOX uptake in K562 and A2780 cell lines

Cell-associated DOX and p-DOX fluorescences were quantified by flow cytometry, by incubating increasing concentrations of the drugs for 90 min with sensitive and resistant K562 and A2780 cells (Fig. 1). Accumulation of DOX was dose dependent and increased in sensitive cells, but was significantly reduced in both resistant cells. The uptake of p-DOX was dose dependent up to 10 μM and then reached a plateau. The uptake of p-DOX was similar in sensitive and resistant K562 cells, suggesting that it bypasses the P-gp. In the A2780 cells, p-DOX seemed to accumulate even more readily in A2780/ADR cells than in sensitive A2780 cells.

We also determined the effect of VPL on the internalization of the drugs in these two cell types (Fig. 1). As expected, addition of VPL to resistant cells led to a marked increase in the accumulation of DOX, as compared to cells treated without VPL. In the case of K562, the levels were restored completely as in the sensitive cells. In contrast, treatment of K562/ADR cells with VPL did not induce any increase in accumulation of p-DOX, confirming that it is not recognized by the P-gp.

Intracellular distribution of p-DOX and DOX in K562 cells

The intracellular distribution of p-DOX and DOX was visualized by confocal microscopy in living sensitive and resistant K562 cells, after 90 min incubation (Fig. 2). In sensitive cells, DOX accumulated intracellularly, mainly in the cytoplasm within vesicular compartments and in the nucleus, whereas p-DOX essentially decorated only nuclear material. In K562/ADR cells, DOX internalization was drastically reduced to a faint punctate, cytoplasmic pattern. As shown earlier, treatment with a P-gp inhibitor, VPL, largely restored DOX uptake in K562/ADR cells. In contrast, p-DOX internalization was equivalent in sensitive and resistant cells, and was unaffected by VPL, indicating that p-DOX internalization is not affected by P-gp overexpression.

Copyright © Lippincott Williams & Wilkins. Unauthorized reproduction of this article is prohibited.

Fig. 1

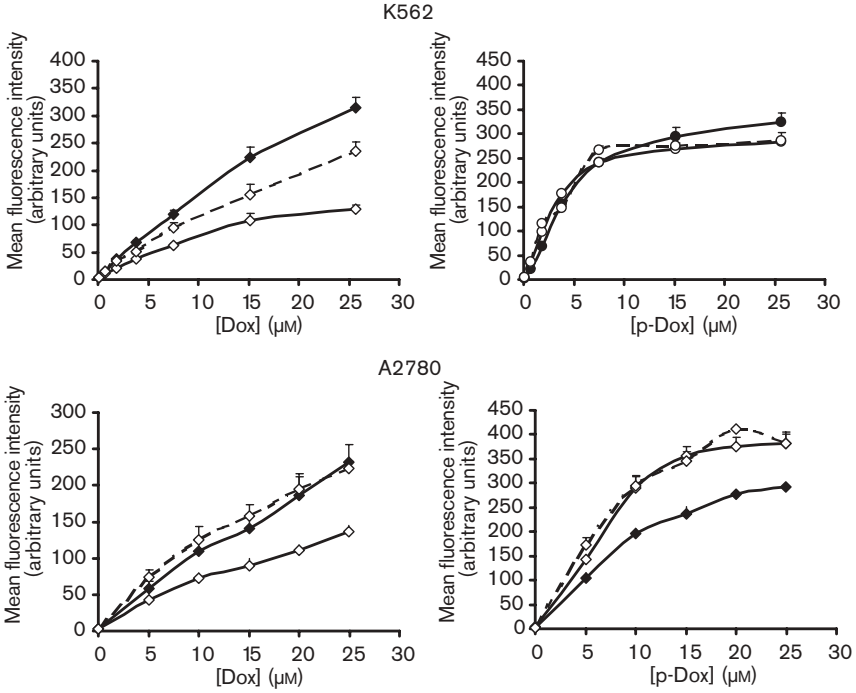

Flow cytometry analysis of DOX and p-DOX internalization in K562 or A2780 cell lines. Increasing concentrations of drugs were incubated for 90 min with sensitive (closed labels) or resistant (open labels) cells, in the absence (straight lines) or presence (dotted lines) or 10 μM VPL, as described in Materials and methods. Internalized drugs were excited at 488 nm and fluorescence was measured at 525 nm. A histogram of fluorescence intensity per cell (1×10^4 counts) was obtained and the calculated mean of this distribution was considered as representative of the amount of intracellular anti-neoplastic agent. Data are the mean ± SEM of three to eight separate experiments.

Intracellular distribution of p-DOX and DOX in A2780 cells

The intracellular distribution of DOX and p-DOX was also compared in living adherent sensitive and resistant A2780 cells (Fig. 3). As observed in K562 cell lines, uptake of DOX was greatly reduced in A2780/ADR cells and was enhanced when resistant cells were treated with VPL. DOX localization appeared to be mainly in the nucleus. Interestingly, p-DOX uptake in A2780 sensitive and resistant cells was also nuclear and independent of VPL treatment. These results are consistent with those obtained using flow cytometry.

In vitro cytotoxicity of p-DOX in sensitive and resistant cells

Cytotoxicity of DOX and p-DOX on sensitive and resistant K562 and A2780 cell lines was investigated after 48 h incubation (Table 1). The p-DOX EC_{50} was 0.61 ± 0.20 nM in K562 cells and 0.25 ± 0.08 nM in A2780 cells, whereas for DOX the EC_{50} values were 144 ± 13 nM in K562 cells and 27.9 ± 6.25 nM in A2780 cells. p-DOX was therefore 236- and 111-fold more potent, respectively, than DOX for triggering cell death in the parental, sensitive cell lines K562 and A2780. As expected, DOX was less potent in the resistant cells than in the parental sensitive cell lines. In K562/ADR and A2780/ADR cells, VPL partially reversed the lack of cytotoxic potency of DOX. In contrast, p-DOX potency was not affected and was completely unchanged by VPL treatment in K562 cells.

Maximal cell death induced by DOX and p-DOX on sensitive K562 and A2780 cells (Table 2) was between 80 and 98%. While E_{max} induced by p-DOX was not different in sensitive versus resistant cells, DOX was 2-fold less potent in resistant cells, as E_{max} decreased to 45.9 ± 3.6% cell death and 53.6 ± 2.4% in K562/ADR and A2780/ADR, respectively. Inhibition of P-gp by VPL completely reversed this lack of efficacy in both types of cell line.

In vitro cytotoxicity of vectorized p-DOX (p-DOX-SynB3)

We coupled p-DOX with the SynB vector, SynB3, via a succinate linker and assessed its internalization and cytotoxic effect. Confocal microscopy showed that p-DOX-SynB3 had a similar pattern of accumulation to that of free p-DOX (data not shown). *In vitro* cytotoxicity studies showed that p-DOX-SynB3 was also significantly more potent than DOX but slightly less cytotoxic than free p-DOX (Table 1). However, its potency was not

Copyright © Lippincott Williams & Wilkins. Unauthorized reproduction of this article is prohibited.

Fig. 2

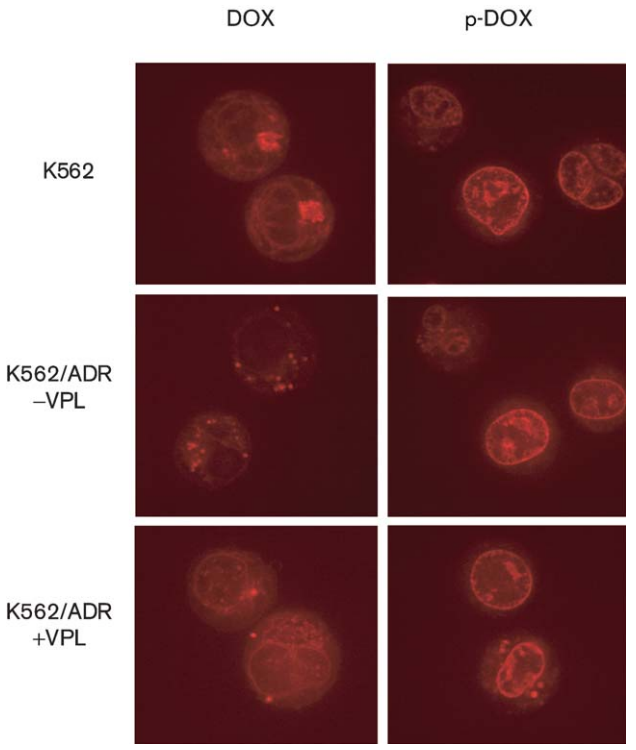

Confocal analysis of DOX (left panel) and p-DOX (right panel) intracellular localization in K562 and K562/ADR cells in the absence (–VPL) or presence (+VPL) of 10 μM VPL. Drugs (25 μM) were incubated with K562 or K562/ADR in Opti-MEM medium at 37°C for 90 min. Cells were then washed with ice-cold PBS, prior to being plated on glass slides and immediately observed without fixation, as precisely described in Materials and methods. Confocal images were obtained with a DMR-B Leica microscope equipped with an Ar-Kr ion laser with excitation line at 488 nm and emission at 525 nm.

Fig. 3

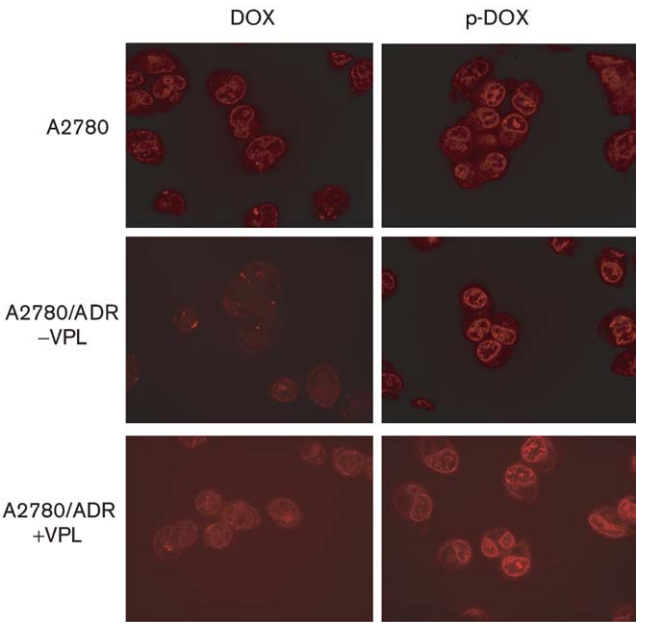

Confocal analysis of DOX (left panel) and p-DOX (right panel) intracellular localization in A2780 and A2780/ADR cells in the absence (–VPL) or presence (+VPL) of 10 μM VPL. Drugs (25 μM) were incubated with A2780 or A2780/ADR, grown on glass slides, in Opti-MEM medium at 37°C for 90 min. Cells were then washed with ice-cold PBS, prior to being immediately observed without fixation. Confocal images were obtained with a DMR-B Leica microscope equipped with an Ar-Kr ion laser with excitation line 488 nm and emission at 525 nm.

affected by VPL treatment in K562 cell lines (Tables 1 and 2). This suggests that the vectorized p-DOX also bypasses the P-gp.

Discussion

This study describes cellular accumulation, intracellular distribution and cytotoxicity of p-DOX, an anthracycline derivative, and its vectorized form in two DOX-resistant cell lines. p-DOX was able to bypass a marked drug resistance in both cell lines. Cellular resistance to cancer chemotherapeutic agents is one of the major obstacles encountered during cancer therapy. This resistance is frequently associated with MDR1 protein (P-gp) overexpression. P-gp belongs to the ATP-binding cassette (ABC) family of transporters, whose members share sequence and structural homology. Both K562/ADR and A2780/ADR cells overexpress the *mdr1* gene product, i.e. P-gp, since flow cytometry analysis of MDR1 expression with fluorescently labeled antibodies showed that more than 90% of K562/ADR or A2780/ADR express P-gp (data not shown).

p-DOX is a potent analog of DOX, described by Nagy *et al.* [40] as being 500–1000 times more potent than its parent compound, DOX, in human breast cancer cell line MCF-7 and mouse mammary carcinoma cells MXT. p-DOX–peptidic hormones conjugates were also designed, and evaluated to trigger targeted cytotoxic effects *in vitro* [42] and *in vivo* [43–45]. However, the ability of p-DOX to bypass cellular resistance, as well as its intracellular accumulation in sensitive and resistant cells, was not investigated.

In this study, we show that p-DOX accumulated to the same extent in sensitive and resistant K562 cells, in contrast to its parental drug DOX, for which cellular accumulation in resistant cells was greatly reduced. Moreover, p-DOX intracellular localization in living cells appeared to be essentially nuclear in sensitive cells, whereas DOX decorated both cytoplasmic and nuclear compartments. Similarly, in A2780/ADR cells, p-DOX internalization was as important as in sensitive A2780, whereas DOX accumulation was greatly reduced. VPL acts both as an inhibitor of drug transport by P-gp and as a stimulator of P-gp-associated ATPase activity, thus resulting in an uncoupling of transport and ATP hydrolysis [47]. VPL and anthracycline interactions with

Copyright © Lippincott Williams & Wilkins. Unauthorized reproduction of this article is prohibited.

Table 1 **Cytotoxic potency in K562 and A2780 cell lines (EC_{50}, nM)**

	K562	K562/ADR		A2780	A2780/ADR	
		− VPL	+ VPL		− VPL	+ VPL
DOX	144 ± 13	5269 ± 653	2572 ± 628[a]	27.91 ± 6.25	768 ± 114	491 ± 102
p-DOX	0.61 ± 0.20	0.33 ± 0.07	0.33 ± 0.07	0.25 ± 0.08	0.48 ± 0.08	0.47 ± 0.08
p-DOX-SynB3	2.29 ± 0.70	1.82 ± 0.32	1.22 ± 0.13	1.44 ± 0.70	6.43 ± 0.53	6.98 ± 0.64

Cells were cultured for 48 h with increasing drug concentrations. Cell viability was assessed by the MTT assay, as described in Materials and methods. EC_{50}s were calculated from complete dose–response curves. Data are the mean ± SEM of four to eight independent experiments, each performed 6 times. Statistical significance between VPL-treated and untreated values was assessed by Student's *t*-test,
[a]$p < 0.05$.

Table 2 **Cytotoxic efficacy in K562 and A2780 cell lines (E_{max},% cell death)**

	K562	K562/ADR		A2780	A2780/ADR	
		− VPL	+ VPL		− VPL	+ VPL
DOX	80.1 ± 5.1	45.9 ± 3.6	83.4 ± 2.6[a]	84.1 ± 12.4	53.6 ± 2.4	91.6 ± 0.8[a]
p-DOX	90.6 ± 0.6	94.4 ± 0.7	92.5 ± 0.4	94.9 ± 1	93.5 ± 0.9	93.4 ± 0.9
p-DOX-SynB3	91.14 ± 0.8	94.4 ± 0.4	94.3 ± 1.0	98.1 ± 0.8	95.2 ± 0.5	92.3 ± 2.1

Cells were cultured for 48 h with increasing drug concentrations. Cell viability was assessed by the MTT assay, as described in Materials and methods. E_{max}s were calculated from complete dose–response curves. Data are the mean ± SEM of four to eight independent experiments, each performed 6 times. Statistical significance between VPL-treated and untreated data was assessed by Student's *t*-test,
[a]$p < 0.05$.

P-gp are thought to be non-competitive [48,49]. As expected, the presence of 10 μM VPL enhanced DOX internalization in both K562/ADR and A2780/ADR cells, whereas p-DOX uptake was not further increased by VPL.

Quantification of intracellular anthracycline fluorescence by flow cytometry also showed that DOX uptake was diminished in both K562/ADR and A2780/ADR cells, in comparison to their sensitive counterparts, and that this effect was partially or totally reversed by the addition of VPL. In contrast, p-DOX internalization was equal in sensitive and resistant cells, and remained unaffected by VPL treatment. Altogether, these results strongly suggest that p-DOX is not a substrate for P-gp and that its accumulation into resistant cell nuclei is at least identical in P-gp-expressing cells compared to sensitive cells.

We observed that treatment of A2780/ADR cells with VPL completely restored DOX uptake, but the *in vitro* potency was only weakly enhanced. This could be explained by two possibilities. (i) The total fluorescence measured by flow cytometry does not reflect the actual intracellular drug content, since anthracycline fluorescence is known to be quenched upon binding to base pairs of DNA [50,51]. (ii) VPL inhibition of DOX uptake is progressively relieved during the 48-h incubation with cells, upon continuous challenge with DOX. Such a resumed active efflux of anthracycline upon long-term incubation with VPL has previously been described [49]. More generally, a lack of correlation between cellular accumulation and cytotoxicity was already reported in previous studies with morpholinyl and methoxypiperidyl derivates of daunorubicin in human cell lines [52,53].

p-DOX and its vectorized form p-DOX-SynB3 were 230 and 63 times more potent than DOX in K562 cells, respectively, and 111 and 19 times more potent than DOX in A2780 cells, respectively. Moreover, p-DOX and p-DOX-SynB3 were as potent to induce K562 and K562/ADR cell death, although in A2780/ADR cells, a slight, but not significant increase was observed in p-DOX potency.

The lack of recognition by P-gp of p-DOX and p-DOX-SynB3 could be explained by the modification of the amino moiety of DOX, which is here included in a pyrrolino ring. The important role of this functional group of DOX in its binding to P-gp has been evidenced by Priebe *et al.* [54] and was also illustrated by the bypass of cellular resistance by another DOX derivative methoxymorpholino-DOX [55], also modified on the same amino group.

The present study demonstrates that p-DOX is not a substrate of the P-gp pump, providing excellent prospects for the treatment of resistant forms of various cancers. Furthermore, the vectorized form of p-DOX (p-DOX-SynB3) retains this useful property. Although p-DOX is more potent *in vitro* than its parent drug DOX [40], it has been found to be toxic *in vivo*. Nagy *et al.* have attempted to reduce the toxicity of the drug employing in particular peptide conjugates targeting specific receptors [41–43]. Here, we have used a member of the SynB peptide family which has been proved to transport effectively several drug-like molecules through the BBB [31,32]. The modification of the pharmacokinetic properties of p-DOX by vectorization is expected to lead to a highly potent and non-toxic compound. Toward this goal, future

Copyright © Lippincott Williams & Wilkins. Unauthorized reproduction of this article is prohibited.

studies are ongoing to explore the anti-tumor potential of the conjugate *in vivo* in brain tumor models.

Acknowledgments

Imaging was performed at the Integrated Imaging Facility of IFR24 (Montpellier). We thank Dr P. Travo, Head of the Facility, for constant interest and support. We are also indebted to C. Rebouissou, responsible of the FACS facilities at the Institut de Génétique Moléculaire. Finally, we would like to thank Dr P. Mouchet and Professor M. Lemaire for helpful advice.

References

1 Juliano RL, Ling V. A surface glycoprotein modulating drug permeability in Chinese hamster ovary cell mutants. *Biochim Biophys Acta* 1976; **455**: 152–162.
2 Gottesman MM, Pastan I. Biochemistry of multidrug resistance mediated by the multidrug transporter. *Annu Rev Biochem* 1993; **62**:385–427.
3 Cordon-Cardo C, O'Brien JP, Casals D, Rittman-Grauer L, Biedler JL, Melamed MR, *et al.* Multidrug-resistance gene (P-glycoprotein) is expressed by endothelial cells at blood–brain barrier sites. *Proc Natl Acad Sci USA* 1989; **86**:695–698.
4 Zaman GJ, Flens MJ, van Leusden MR. The human multidrug resistance-associated protein MRP is a plasma membrane drug-efflux pump. *Proc Natl Acad Sci USA* 1994; **91**:8822–8826.
5 Chamberlain MC, Khatibi S, Kim JC, Howell SB, Chatelut E, Kim S. Treatment of leptomeningeal metastasis with intraventricular administration of depot cytarabine (DTC 101). A phase I study. *Arch Neurol* 1993; **50**:261–264.
6 Kroll RA, Neuwelt EA. Outwitting the blood–brain barrier for therapeutic purposes Osmotic opening and other means. *Neurosurgery* 1998; **42**:1083–1099.
7 Bartlett NL, Lum BL, Fisher GA. Phase I trial of doxorubicin with cyclosporine as a modulator of multidrug resistance. *J Clin Oncol* 1994; **12**:835–842.
8 Shoji Y, Fisher MH, Periasamy A, Herman B, Juliano RL. Verapamil and cyclosporin A modulate doxorubicin toxicity by distinct mechanisms. *Cancer Lett* 1991; **57**:209–218.
9 Pommerenke E, Mattern J, Volm M. Modulation of doxorubicin-toxicity by tamoxifen in multidrug-resistant tumor cells *in vitro* and *in vivo*. *J Cancer Res Clin Oncol* 1994; **120**:422–426.
10 Kusunoki N, Takara K, Tanigawara Y. Inhibitory effects of a cyclosporin derivative, SDZ PSC 833, on transport of doxorubicin and vinblastine via human P-glycoprotein. *Jpn J Cancer Res* 1999; **89**:1220–1228.
11 Firestone RA, Pisano JM, Falck JR, McPhaul MM, Krieger M. Selective delivery of cytotoxic compounds to cells by the LDL pathway. *J Med Chem* 1984; **27**:1037–1043.
12 Masquelier M, Vitols S, Peterson C. Low-density lipoprotein as a carrier antitumoral drugs: *in vivo* fate of drug–human low-density lipoprotein complexes in mice. *Cancer Res* 1986; **46**:3842–3847.
13 Dosio F, Brusa P, Crosasso P, Arpicco S, Cattel L. Preparation, characterization and properties *in vitro* and *in vivo* of a paclitaxel–albumin conjugate. *Journal of Controlled Release* 1997; **47**:293–304.
14 Kratz F, Beyer U, Schumacher P, Krüger M, Zahn H, Roth T, *et al.* Synthesis of new maleimide derivatives of daunorubicin and biological activity of acid labile transferrin conjugates. *Bioorg Med Chem Lett* 1997; **7**:617–622.
15 Greenfield RS, Senter PD, Daues A, Fitzgerald KA, Gawlak S, Manger W, *et al. In vitro* evaluation of immunoconjugates prepared by linking mitomycin C to monoclonal antibodies via polyglutamic acid carriers. *Antibody Immunoconj Radiopharm* 1989; **2**:201–216.
16 Hinman LM, Hamann PR, Wallace R, Menendez AT, Durr FE, Upeslacis J. Preparation and characterization of monoclonal antibody conjugates of the calicheamicins: a novel and potent family of antitumor antibiotics. *Cancer Res* 1993; **53**:3336–3342.
17 Kulkarni PN, Blair AH, Ghose T. Covalent binding of methotrexate to immunoglobulins and the effect of antibody-linked drug on tumor growth *in vivo*. *Cancer Res* 1981; **41**:2700–2706.
18 Smyth MJ, Pietersz GA, Classon BJ, McKenzie FC. Specific targeting of chlorambucil to tumors with the use of monoclonal antibodies. *J Natl Cancer Inst* 1986; **76**:503–510.
19 Choi WM, Kopeckova P, Minko T, Kopecek J. Synthesis of HPMA copolymer containing adriamycin bound via an acid-labile spacer and its activity toward human ovarian carcinoma cells. *J Bioactive Compatible Polym* 1999; **14**:447–456.
20 Duncan R, Gac-Breton S, Keane R, Musila R, Sat YN, Satchi R, *et al.* Polymer–drug conjugates, PDEPT and PELT: basic principles for design and transfer from the laboratory to clinic. *J Controlled Rel* 2001; **74**:135–146.
21 Gianasis E, Wasil M, Evagorou EG, Keddle A, Wilson G, Duncan R. HPMA Copolymer platinates as novel antitumor agents: *in vitro* properties, pharmacokinetics and antitumour activity *in vivo*. *Eur J Cancer* 1999; **35**:994–1002.
22 Hurwitz E, Wilchek M, Pitha J. Soluble macromolecules as carriers for daunorubicin. *J Appl Biochem* 1980; **2**:25–35.
23 Nichifor M, Schacht EH, Seymour LW. Polymeric prodrugs of 5-fluorouracil. *J Controlled Rel* 1997; **48**:165–718.
24 Subr V, Strohalm J, Ulbrich K, Duncan R, Hume IC. Polymers containing enzymatically degradable bonds, XII. Effect of spacer structure on the rate of release of daunomycin and adriamycin from poly[*N*-(2-hydroxypropyl)-methacrylamide] copolymer drug carriers *in vitro* and antitumor activity measured *in vivo*. *J Controlled Rel* 1992; **18**:123–132.
25 Matsumoto S, Yamamoto A, Takakura Y, Hashida M, Sezaki H. Cellular interaction and *in vitro* antitumor activity of mitomycin C-dextran conjugate. *Cancer Res* 1986; **46**:4463–4468.
26 Felgner JH, Kumar R, Sridhar CN, Wheeler CJ, Tsai YJ, Border R, *et al.* Enhanced gene delivery and mechanism studies with a novel series of cationic lipid formulation. *J Biol Chem* 1994; **269**:2550–2561.
27 Harding JA, Engbers CM, Newman MS, Goldstein NI, Zalipsky S. Immunogenicity and pharmacokinetic attributes of poly(ethylene glycol)-grafted immunoliposomes. *Biochim Biophys Acta* 1997; **1327**:181–192.
28 Selvam MP, Buck SM, Blay RA, Mayner RE, Mied PA, Epstein JS. Inhibition of HIV replication by immunoliposomal antisense oligonucleotide. *Antiviral Res* 1996; **33**:11–20.
29 Soma CE, Dubernet C, Barratt G, Nemati F, Appel M, Benita S, *et al.* Ability of doxorubicin-loaded nanoparticles to overcome multidrug resistance of tumor cells after their capture by macrophages. *Pharm Res* 1999; **16**:1710–1716.
30 Cserhati T, Forgags E, Hollo J. Interaction of taxol and other anticancer drugs with α-cyclodextrin. *J Pharm Biomed Anal* 1995; **13**:533–541.
31 Rousselle C, Clair P, Lefauconnier JM, Kaczorek M, Scherrmann JM, Temsamani J. New advances in the transport of doxorubicin through the blood–brain barrier by a peptide vector-mediated strategy. *Mol Pharmacol* 2000; **57**:679–686.
32 Rousselle C, Clair P, Smirnova M, Kolesnikov Y, Pasternak GW, Gac-Breton S, *et al.* Improved brain uptake and pharmacological activity of dalargin using a peptide-vector-mediated strategy. *J Pharmacol Exp Ther* 2003; **306**: 371–376.
33 Rousselle C, Smirnova M, Clair P, Lefauconnier JM, Chavanieu A, Calas B, *et al.* Enhanced delivery of doxorubicin into brain via a peptide-vector mediated strategy: saturation kinetics and specificity. *J Pharmacol Exp Ther* 2001; **296**:124–131.
34 Mazel M, Clair P, Rousselle C, Vidal P, Scherrmann JM, Mathieu D, *et al.* Doxorubicin–peptide conjugates overcome multidrug resistance. *Anticancer Drugs* 2001; **12**:107–116.
35 Acton EM, Tong GL, Mosher CW, Wolgemuth RL. Intensely potent morpholinyl anthracyclines. *J Med Chem* 1984; **27**:638–645.
36 Sikic BL, Ehsan MN, Harker VG, Friend NF, Brown BW, Newman RA, *et al.* Dissociation of antitumor potency from anthracycline cardiotoxicity in a doxorubicin analog. *Science* 1985; **228**:1544–1546.
37 Zwelling LA, Altshuler E, Cherif A, Farquhar D. *N*-(5,5-diacetoxypentyl)doxorubicin: a novel anthracycline producing DNA interstrand cross-linking and rapid endonucleolytic cleavage in human leukemia cells. *Cancer Res* 1991; **51**:6704–6707.
38 Lau DH, Duran GE, Sikic BI. Characterization of covalent DNA binding of morpholino and cyanomorpholino derivatives of doxorubicin. *J Natl Cancer Inst* 1992; **84**:1587–1592.
39 Lewis AD, Lau DH, Duran GE, Wolf CR, Sikic BI. Role of cytochrome P-450 from the human CYP3A gene family in the potentiation of morpholino doxorubicin by human liver microsomes. *Cancer Res* 1992; **52**:4379–4384.
40 Nagy A, Armatis P, Schally AV. High yield conversion of doxorubicin to 2-pyrrolinodoxorubicin, an analog 500–1000 times more potent: structure–activity relationship of daunosamine-modified derivatives of doxorubicin. *Proc Natl Acad Sci USA* 1996; **93**:2464–2469.
41 Nagy A, Schally AV, Armatis P, Szepeshazi K, Halmos G, Kovacs M, *et al.* Cytotoxic analogs of luteinizing hormone-releasing hormone containing doxorubicin or 2-pyrrolinodoxorubicin, a derivative 500–1000 times more potent. *Proc Natl Acad Sci USA* 1996; **93**:7269–7273.
42 Nagy A, Armatis P, Cai RZ, Szepeshazi K, Halmos G, Schally AV. Design, synthesis, and *in vitro* evaluation of cytotoxic analogs of bombesin-like

Copyright © Lippincott Williams & Wilkins. Unauthorized reproduction of this article is prohibited.

peptides containing doxorubicin or its intensely potent derivative, 2-pyrrolinodoxorubicin. *Proc Natl Acad Sci USA* 1997; **94**:652–656.
43 Nagy A, Schally AV, Halmos G, Armatis P, Cai RZ, Csernus V, *et al.* Synthesis and biological evaluation of cytotoxic analogs of somatostatin containing doxorubicin or its intensely potent derivative, 2-pyrrolinodoxorubicin. *Proc Natl Acad Sci USA* 1998; **95**:1794–1799.
44 Kiaris H, Schally AV, Nagy A, Sun B, Szepeshazi K, Halmos G. Regression of U-87 MG human glioblastomas in nude mice after treatment with a cytotoxic somatostatin analog AN-238. *Clin Cancer Res* 2000; **6**:709–717.
45 Plonowski A, Schally AV, Nagy A, Sun B, Szepeshazi K. Inhibition of PC-3 human androgen-independent prostate cancer and its metastases by cytotoxic somatostatin analogue AN-238. *Cancer Res* 1999; **59**: 1947–1953.
46 Atherton E, Sheppard RC. Reaction procedures and operating techniques. In: Rickwood D, Hames BD (editors): *Solid Phase Peptide Synthesis: A Practical Approach*. Oxford: IRL Press; 1989, pp. 131–137.
47 Litman T, Druley TE, Stein WD, Bates SE. From MDR to MXR: new understanding of multidrug resistance systems, their properties and clinical significance. *Cell Mol Life Sci* 2001; **58**:931–959.
48 Spoelstra EC, Westerhoff HV, Pinedo HM, Dekker H, Lankelma J. The multidrug-resistance-reverser verapamil interferes with cellular P-glycoprotein-mediated pumping of daunorubicin as a non-competing substrate. *Eur J Biochem* 1994; **221**:363–373.
49 Litman T, Zeuthen T, Skovsgaard T, Stein WD. Competitive, non-competitive and cooperative interactions between substrates of P-glycoprotein as measured by its ATPase activity. *Biochim Biophys Acta* 1997; **1361**: 169–176.
50 Tarasiuk J, Frezard F, Garnier-Suillerot A, Gattegno L. Anthracycline incorporation in human lymphocytes. Kinetics of uptake and nuclear concentration. *Biochim Biophys Acta* 1989; **1013**:109–117.
51 Praet M, Stryckmans P, Ruysschaert JM. Cellular uptake, cytotoxicity, and transport kinetics of anthracyclines in human sensitive and multidrug-resistant K562 cells. *Biochem Pharmacol* 1996; **51**:1341–1348.
52 Johnston JB, Glazer RI. Pharmacological studies of 3′-(4-morpholinyl)-3′-deaminodaunorubicin in human colon carcinoma cells *in vitro*. *Cancer Res* 1983; **43**:1044–1048.
53 Johnston JB, Glazer RI. Cellular pharmacology of 3′-(4-morpholinyl) a nd 3′-(4-methoxy-1-piperidinyl) derivatives of 3′-deaminodaunorubicin in human colon carcinoma cells *in vitro*. *Cancer Res* 1983; **43**:1606–1610.
54 Priebe W, Van NT, Burke TG, Perez-Soler R. Removal of the basic center from doxorubicin partially overcomes multidrug resistance and decreases cardiotoxicity. *Anticancer Drugs* 1993; **4**:37–48.
55 Bakker M, Renes J, Groenhuijzen A, Visser P, Timmer-Bosscha H, Muller M, *et al.* Mechanisms for high methoxymorpholino doxorubicin cytotoxicity in doxorubicin-resistant tumor cell lines. *Int J Cancer* 1997; **73**:362–366.

Copyright © Lippincott Williams & Wilkins. Unauthorized reproduction of this article is prohibited.